***JKPK (JURNAL KIMIA DAN PENDIDIKAN KIMIA)**, Vol. 7, No. 1, 2022* *pp. 1-11*
Chemistry Education Study Program, Universitas Sebelas Maret *ISSN 2503-4146*
https://jurnal.uns.ac.id/jkpk *ISSN 2503-4154 (online)*

CHARACTERIZATION OF VANADIUM-DOPED $BaBi_4Ti_4O_{15}$ PREPARED BY MOLTEN KCl SALT METHOD

Suci Noerfaiqotul Himmah, Puspa Sari, and Anton Prasetyo*

Department of Chemistry, Faculty of Science and Technology, Universitas Islam Negeri Maulana Malik Ibrahim Malang
Jl. Gajayana No. 50, Malang, 65144, Indonesia

* Correspondence email: anton@kim.uin-malang.ac.id

Received: December 12, 2020 Accepted: April 18, 2022 Online Published: April 30, 2022
DOI : 10.20961/jkpk.v7i1.58661

ABSTRACT

One of the potential properties of the Aurivillius compound is photocatalyst. The four-layered Aurivillius compound $BaBi_4Ti_4O_{15}$ has a bandgap energy of 3.2 eV caused having work function in the UV light area. The strategy to decrease the bandgap energy is doping with metal elements such as vanadium (V). In this research, vanadium-doped $BaBi_4Ti_4O_{15}$ ($BaBi_4Ti_{4-x}V_xO_{15}$) (x= 0, 0.05, 0.1, and 0.15)) compounds was synthesized through the molten KCl salt method. The diffractogram samples showed that $BaBi_4Ti_{4-x}V_xO_{15}$ (x= 0, 0.05, 0.1, 0.15) had been successfully obtained but still found impurities: (a) TiO_2 (rutile phase) at x= 0, 0.05, 0.1, 0.15, and (b) $Bi_4V_2O_{11}$ at x= 0.15. The SEM image showed that the particle has plate-like morphology. The UV-Vis DRS spectrum showed that vanadium-doped $BaBi_4Ti_4O_{15}$ has lower bandgap energy.

***Keywords**: $BaBi_4Ti_4O_{15}$, molten KCl Salt, photocatalyst, vanadium*

INTRODUCTION

The Aurivillius family of bismuth-based layered structures ferroelectrics (BLSF) are compounds with the general formula $Bi_2A_{m-1}B_mO_{3m+3}$ with m (1, 2, 3, 4,…..) is an integer indicating the number of perovskite layers. The compound with the structure of Aurivillius is arranged alternately by a bismuth layer $(Bi_2O_2)^{2+}$ and a perovskite layer $(A_{m-1}B_mO_{3m+3})^{2-}$. *A*-cation is a larger-sized cation such as Na^+, Mg^{2+}, Sr^{2+}, Ba^{2+}, and Bi^{3+}, while *B*-cation is a transition metal cation smaller than metal *A*-cation and has a high charge such as Ti^{4+}, Nb^{5+}, Ta^{6+}, and V^{5+} [1]. Many interesting properties of Aurivillius compounds have been reported, such as ferroelectricity [2], photoluminescence [3], photocatalyst [4], and thermoelectricity [5]. The BLSF exhibits superior photocatalytic activity, which correlates with: (a) existence of a hybridized valence band consisting of Bi 6*s* and O 2*p* states which induce the absorption of band edge, thereby induce to a reduction of the bandgap energy [6]; and (b) increasing the mobility of photoexcitation holes [7, 8]. The potential utilization of photocatalysis technology can be found in the following fields such as the production of H_2 through the water-splitting process (water photolysis), the production of CH_4 through CO_2 reduction, photodecomposition, or

photooxidation of harmful substances, artificial photosynthesis, photoinduction super hydrophilicity [9]. Aurivillius compounds have been reported to have photocatalytic activity, such as $Bi_5Ti_3FeO_{15}$ [10], $Bi_4Ti_3O_{12}$ [11], $K_2La_2Ti_3O_{10}$ [12].

$BaBi_4Ti_4O_{15}$ is a four-layered Aurivillius compound which reported to have orthorhombic structure with the space group $A2_1am$ at low temperatures and tetragonal at high temperatures with the space group $I4/mmm$ [13, 14]. $BaBi_4Ti_4O_{15}$ compound was reported to have interesting properties, such as dielectric, piezoelectric [15], ferroelectric [16], and photocatalytic properties [17]. As a photocatalyst material, $BaBi_4Ti_4O_{15}$ has a bandgap energy of 3.2 eV (387.76 nm); in consequence active in the ultraviolet light region due to its large intrinsic bandgap energy and is less profitable in using an excitation source from sunlight. The components of the solar spectrum only contain ultraviolet (UV) rays, as much as 3.5% of the spectrum. At the same time, most of the sun's spectrum consists of visible light 48% and near-infrared (NIR) 44% [18]. Therefore, a strategy is needed to reduce the bandgap energy of $BaBi_4Ti_4O_{15}$ and thus can be activated under visible light. Transition metal doping to photocatalyst compound is a strategy to extend the light absorption to the visible [19]. Some metals that have been reported to be used as dopant are La [20], Nb [21], Fe [22], Cr [23], V [24], and Eu [25].

Several researchers have reported the use of vanadium metal as a photocatalyst dopant. Vanadium metal doping on $K_2La_2Ti_{3-x}V_xO_{11}$ (x= 0.0005, 0.01, 0.015, 0.02, and 0.025) reduced the bandgap energy from 4 to 2.1 eV and increased of water splitting activity [12]. Meanwhile, vanadium metal doping on $Bi_4Ti_{3-x}V_xO_{12}$ (x= 0, 0.05, 0.1, 0.15, and 0.2) succeeded in reducing of band gap energy from 2.91 to 1.50 eV [11]. In addition, samarium and vanadium co-doping on $Bi_4Ti_3O_{12}$ succeeded in degrading NO_x compounds by as much as 12% under visible light radiation for 60 minutes and 17% for 120 minutes [26]. Therefore, vanadium has the potential to be used as dopant in photocatalyst materials to increase its photocatalytic activity.

Several synthesis methods of Aurivillius compounds are reported, such as solid-state reaction [27], molten salt [28], sol-gel [29], and hydrothermal [30]. The molten salt synthesis (MSS) method is a powder preparation method that involves using molten salt as a preparation medium [31]. MSS is a green synthesis method that has many advantages over other methods, such as (a) simple method [32], (b) environmentally friendly [33], (c) using relatively lower temperature [34], (d) increasing reaction rate ion diffusion degree of homogeneity (distribution of elemental constituents in solid solution) [35, 36], (e) controlling the particle size and shape [37], and (f) minimizing agglomeration [38], Huang et al. [39] succeeded in synthesizing $BaBi_4Ti_4O_{15}$ compounds using the molten salt method of NaCl-KCl and Na_2SO_4-K_2SO_4 respectively at a temperature of 850°C, and no impurities were found with a homogeneous plate-like morphology without the formation of agglomerations. Therefore, it indicated that the MSS method could be used in synthesizing metal-doped $BaBi_4Ti_4O_{15}$. In

addition, the synthesis of $BaBi_4Ti_4O_{15}$ using the KCl molten salt method has previously been successfully carried out and is reported to produce a small plate-like morphology of $BaBi_4Ti_4O_{15}$, particles [40].

The Previous results of the synthesis of a single crystal compound $BaBi_4Ti_4O_{15}$ doped with vanadium have been reported [40] and showed that it had an effect on ferroelectric properties, while the effect of doping on photocatalyst properties (band gap energy) had not been reported. Therefore, In this research, vanadium-doped $BaBi_4Ti_4O_{15}$ ($BaBi_4Ti_{4-x}V_xO_{15}$ (x= 0, 0.05, 0.1, and 0.15)) was synthesized as purposes to be photocatalyst material and prepared by the molten KCl salt method and characterized by the *X*-ray diffraction (XRD) technique, scanning electron microscope-energy dispersive spectroscopy (SEM-EDS), and ultraviolet-visible diffuse reflectance spectroscopy (UV-Vis DRS).

METHODS

1. Sample Preparation

$BaBi_4Ti_{4-x}V_xO_{15}$ (x= 0, 0.05, 0.1, and 0.15) powder was prepared by molten KCl salt method in a ratio of 1:7. The oxide reagent powder Bi_2O_3 (Sigma Aldrich, 99.9%), $BaCO_3$ (Merck 99.9%), TiO_2 (Sigma Aldrich, 99.9%), V_2O_5 (Sigma Aldrich, 99.9%), KCl (Merck, 99.9%) was mixed in the stoichiometry ratio and ground in a mortar agate for 1 hour while adding acetone. The crushed samples were then put in an alumina crucible and calcined at a temperature of 780 and 820°C for 8 hours. And then, the sample product was cooled to room temperature, then washed with warm water to remove the chlorine salts, and samples were dried in an oven at 80°C for 2 hours

2. Characterization

The samples phase of the product was characterized by XRD (Rigaku Miniflex diffractometer) with Cu Kα radiation 40 kV and 15 mA in the range 2θ = 10-70°. The obtained diffractogram will be matched with the $BaBi_4Ti_4O_{15}$ diffractogram database in JCPDS No. 035-0757 [42]. SEM equipped with EDS (JEOL JSM-636LA) was used to observe particle morphology and determine the elemental composition of compounds. From the image obtained, the morphology of particles before and after doping with vanadium will be compared [43]. The reflectance spectrum analysis used UV-Vis DRS spectrometer Thermo Evolution 220 in the wavelength range of 200-800 nm. Then the spectrum obtained was calculated using the Kubelka-Munk equation to get the bandgap energy, and the band gap energy will be compared between the vanadium-doped and undoped compounds [44].

RESULTS AND DISCUSSION

The diffractogram analysis was carried out to identify the type of compound phase of the sample formed. Figure 1 shows The diffractogram of the $BaBi_4Ti_{4-x}V_xO_{15}$ (x= 0, 0.05, 0.1, and 0,15) and then indexed with the standard $BaBi_4Ti_4O_{15}$ data in the Joint Committee on Powder Diffraction Standards (JCPDS) database No. 035-0757. The results showed that $BaBi_4Ti_4O_{15}$ compound has successfully synthesized but still found additional peaks that correspond to the

secondary phase of rutile TiO_2 for *x*= 0, 0.05, 0.1, and 0.15. It indicated that the reaction had not yet occurred entirely. In addition, another secondary phase was found at *x*= 0.15 due to the tendency of the V doping ion to form an impurity phase when it exceeded its solubility limit [45].

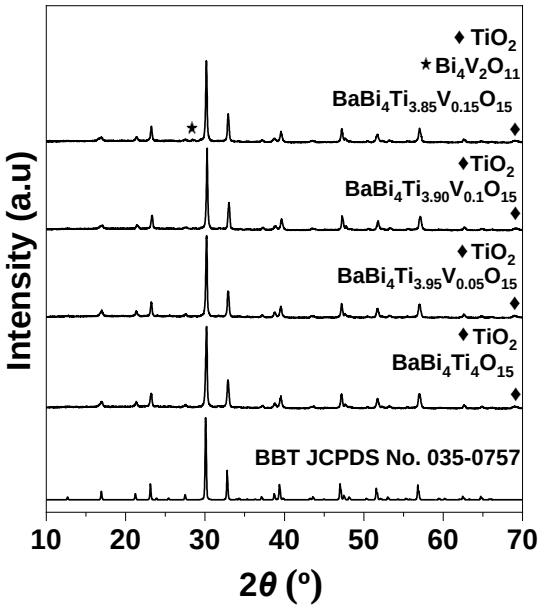

Figure 1. The diffractogram of $BaBi_4Ti_{4-x}V_xO_{15}$ (*x*= 0, 0.05, 0.1, and 0.15)

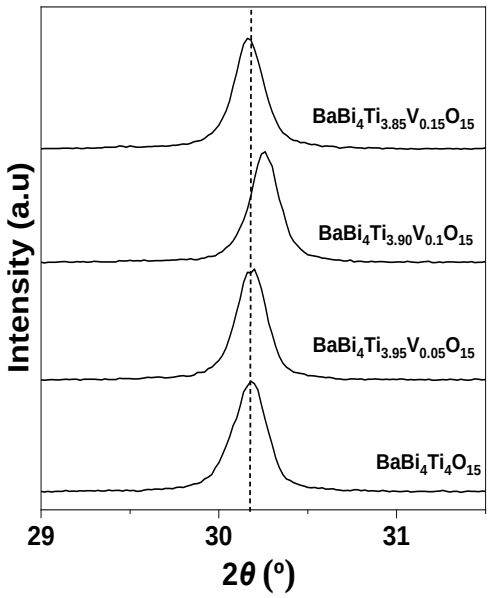

Figure 2. The diffraction peaks shifting on $BaBi_4Ti_{4-x}V_xO_{15}$ (*x*= 0, 0.05, 0.1, and 0.15) at 2*θ*= ~31º

Figure 2 showed peaks shifting at 2*θ* =~31º, indicating a change in lattice parameters and crystal size. It can be seen that the peak position for *x*= 0.1 shifted towards a larger 2*θ* due to V^{5+} (0.46 nm) having a smaller radius than Ti^{4+} (0.53 nm) and decreases an orthorhombic distortion due to the displacement of the cationic center and the adjustment of the slope of oxygen octahedron to reach a new equilibrium due to the substitution of Ti by V [46]. At x= 0.05 and 0.15. There was a minor shift to 2θ because the V dopant was reduced to V^{4+} (0.53 nm) or V^{3+} (0.64 nm) having a larger radius than Ti^{4+}. Another study reported that substitution of V^{3+} on Ti^{4+} caused a shift diffraction peak to a lower value than in the pure state. [47].

Figure **3** showed surface morphology of the four-layered Aurivillius $BaBi_4Ti_{4-x}V_xO_{15}$ (*x*= 0, 0.05, 0.1, and 0.15) compounds. The morphology particles were plate-like and

similar to previous studies [39]. The plate-like morphological characters got better with increasing concentration of V dopant as a result of increasing *c*-axis oriented crystals growth, where plate-like morphology grew in this orientation [48]. However, the formation of agglomeration occurred due to the high degree of saturation and high viscosity of the salt in the diffuse-solution stage [49]. Meanwhile, the elemental composition of samples is tabulated in **Table 1**. It showed that the constituent elements in the sample consisted of Ba, Bi, Ti, V, and O elements. These results also indicated that V dopant was identified in the sample. The V obtained from the EDS analysis increased with increasing V doping concentration.

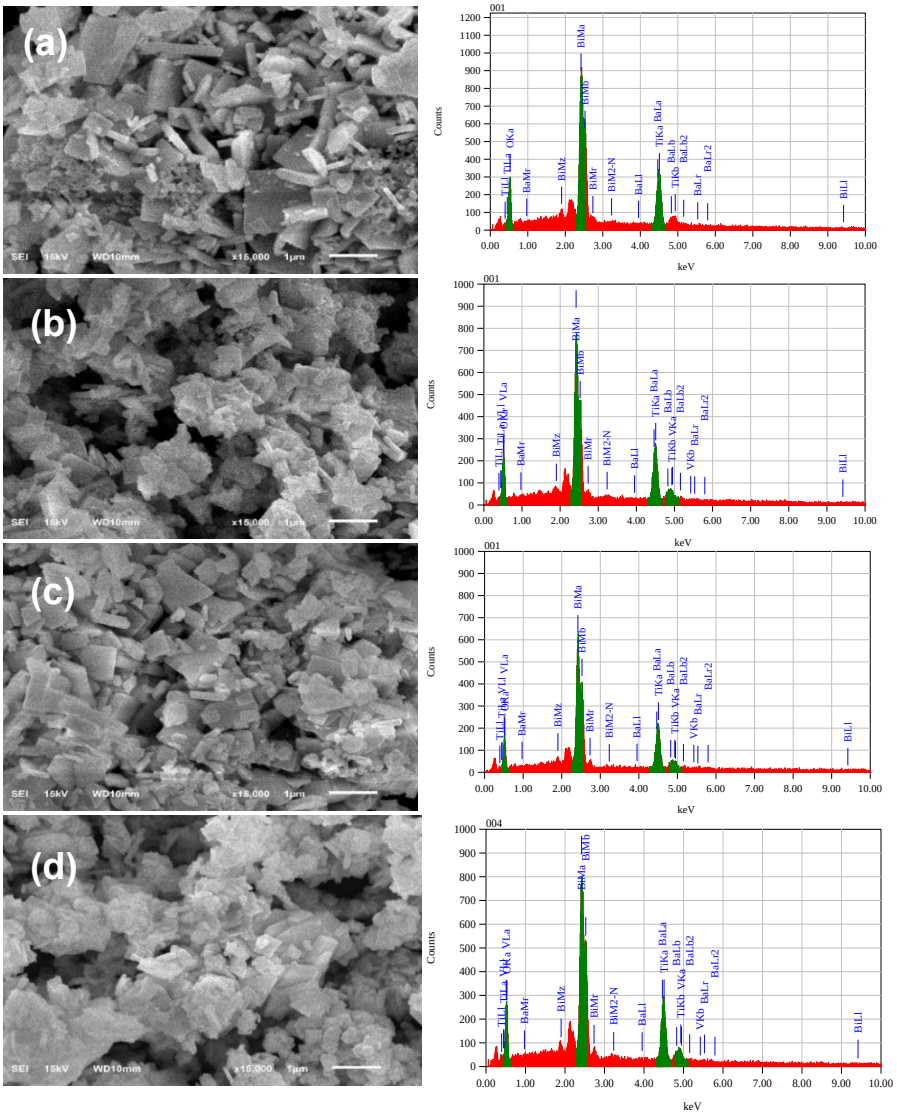

Figure 3. SEM micrograph and EDS spectrum of $BaBi_4Ti_{4-x}V_xO_{15}$ compounds for x= (a) 0, (b) 0.05, (c) 0.1, and (d) 0.15

Table 1. The percentage of constituent elements of $BaBi_4Ti_{4-x}V_xO_{15}$ (x= 0, 0.05, 0.1, and 0.15) compounds

Sample	Ba (%)	Bi (%)	Ti (%)	V(%)	O (%)
$BaBi_4Ti_4O_{15}$	9.67	22.77	19.84	-	47.71

$BaBi_4Ti_{3.95}V_{0.05}O_{15}$	8.99	25.34	20.41	0.31	44.95
$BaBi_4Ti_{3.9}V_{0.1}O_{15}$	10.68	26.43	21.24	1.69	39.96
$BaBi_4Ti_{3.85}V_{0.15}O_{15}$	10.83	22.96	16.35	1.88	47.98

Figure 4 shows the DRS spectrum of % reflectance intensity as a function of wavelength. The % reflectance intensity of samples decreased with increasing V concentration due to the formation of new energy levels V-3*d* below Ti-3*d* in the conduction band. In addition, the V ion strongly affects O due to its higher positive charge and smaller radius than the Ti ion. As a result, the absorption edge of light goes to a longer wavelength [50].

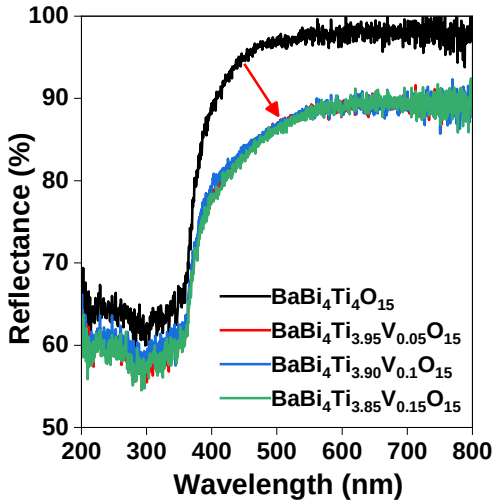

Figure 4. DRS spectra of relationship between % reflectance and wavelength of $BaBi_4Ti_{4-x}V_xO_{15}$ (x= 0, 0.05, 0.1, and 0.15)

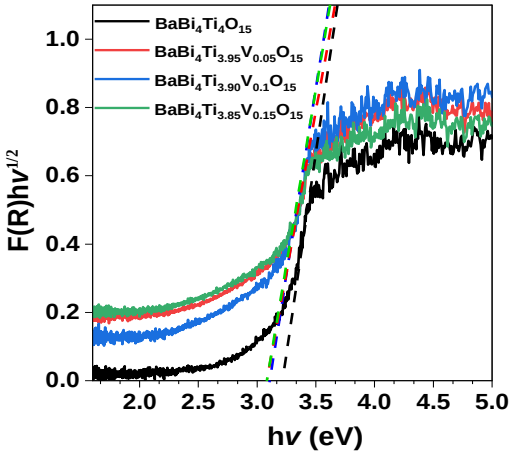

Figure 5. Plot Tauc of $BaBi_4Ti_{4-x}V_xO_{15}$ (x= 0, 0.05, 0.1, and 0.15)

Table 3. The band gap energy of $BaBi_4Ti_{4-x}V_xO_{15}$ (x= 0, 0.05, 0.1, and 0.15)

Sample	Band gap energy (eV)	Wavelength (nm)
$BaBi_4Ti_4O_{15}$	3.20	387.76
$BaBi_4Ti_{3.95}V_{0.05}O_{15}$	3.10	400.27
$BaBi_4Ti_{3.9}V_{0.1}O_{15}$	3.09	401.56

$BaBi_4Ti_{3.85}V_{0.15}O_{15}$	3.09	401.56

The Tauc-plot was calculated by the Kubelka-Munk equation of $BaBi_4Ti_{4-x}V_xO_{15}$ (*x*= 0, 0.05, 0.1; 0.15); the measured reflectance spectrum can be converted into an absorption spectrum by expressing Kubelka-Munk function $(F(R_\infty)$: $(F(R_\infty).hv)^{\frac{1}{\gamma}} = B(hv - E_g)$, with $h, (F(R_\infty)$, v and E_g are Planck's constant, absorption coefficient, photon's frequency, and band gap energy. Meanwhile, *B* is a constant and represents an electronic transition. γ is ½ or 2 depending on the direct and indirect transition of the band gap energy. Figure 5 showed the reflectance spectrum of $BaBi_4Ti_{4-x}V_xO_{15}$ (indirect band gap semiconductor) transformed according to the Kubelka-Munk equation plotted against photon energy. The *x*-intercept of the linear fit of the Tauc plot provides an evaluation of the band gap energy value [44, 51]. The band gap energies obtained for all samples are tabulated in **Table 3**. The band gap energy value of the $BaBi_4Ti_4O_{15}$ compound was 3.2 eV, and it is similar to a previous report by Qi et al. [17]. The band gap energy decreased from 3.2 to 2.09 eV with increasing V doping concentration. As a result, the work function shifted closer to the visible area (redshift).

The decrease of band gap energy is caused by new electronic band structure state due to the substitution of V on Ti. The V element is more electronegative than Ti, causing it to form an interstitial state by the V-3*d* orbital occupied at the lowest edge of the Ti 3*d* conduction band. The interstitial state formed by V-3*d* is about 0.1-0.3 eV below Ti-3*d* [52, 53]. Therefore, it is possible to change the electronic transition from Bi-6*s* + O-2*p* (VB) to Ti-3*d* (CB) orbitals to Bi-6*s* + O-2*p* (VB) to V-3*d* (CB) orbitals with bandgap energy value is lower than in the pure state. The decrease in band gap energy is also caused by increasing the bond order between dopant ion and oxide orbital; the interaction of the V-3*d* and O*p* orbitals becomes stronger due to the smaller radius of V than Ti [54]. The illustration of electronic transition in $BaBi_4Ti_{4-x}V_xO_{15}$ (*x*= 0, 0.05, 0.1, and 0.15) compounds can be proposed in Figure 6. $BaBi_4Ti_{4-x}V_xO_{15}$ (*x*= 0, 0.05, 0.1, and 0.15).

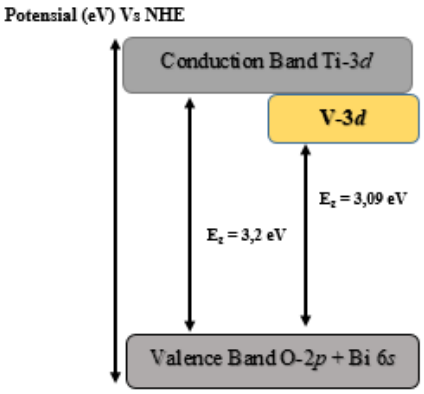

Figure 6. The proposed of illustration of electronic transition in $BaBi_4Ti_{4-x}V_xO_{15}$ (*x*= 0, 0.05, 0.1, 0.15)

CONCLUSION

The four-layered Aurivillius $BaBi_4Ti_{4-x}V_xO_{15}$ (*x*= 0, 0.05, 0.1, 0.15) compounds were successfully synthesized using the KCl molten salt method. Nevertheless, these formed secondary phases at all V concentrations, namely TiO_2 and another secondary phase at *x*= 0.15, which is $Bi_4V_2O_{11}$. All obtained powder has plate-like morphologies. The DRS spectra of the sample showed that V dopant shifted work function closer to the visible wavelength. These results indicate that V dopant formed

a newelectronic state with lower band gap energy.

REFERENCES

[1] B. Aurivillius, "Mixed Bismuth Oxides with Layer Lattices: I The Structure Type of $Bi_4Ti_3O_{12}$," *Arkiv Kemi Band.*, vol. 1, no. 154, pp. 499-512, 1949.

[2] Z. Lazeravic, B. Stojanovic, and J. Varela, "Approach to Analyzing Synthesis, Structure and Properties of Bismuth Titanate Ceramics," *Sci. Sinter.*, vol. 37, no. 3, pp. 199-216, 2005. DOI: 10.2298/SOS0503199L

[3] D. Peng, H. Zou, C. Xu, X. Wang, and X. Yao, "Er Doped $BaBi_4Ti_4O_{15}$ Multifunctional Ferroelectrics: Up-Conversion Photoluminescence, Dielectric and Ferroelectric Properties," *J. Alloys Compd*., vol. 552, pp. 463-468, 2013. DOI:10.1016/J.JALLCOM.2012.10.194

[4] W. F. Yao, H. Wang, X. H. Xu, Y. Huo, Y. Zhang, and M. Wang, "Synthesis and Photocatalytic Property of Bismuth Titanate $Bi_4Ti_3O_{12}$," *Mater. Lett.*, vol. 57, no. 13, pp. 1899-1902, 2003. DOI: 10.1016/S0167-577X(02)01097-2

[5] H. Kohri and T. Yagasaki, "Thermoelectric Generating Properties of Aurivillius Compounds," *Adv. Sci. Tech*., vol. 77, pp. 285-290, 2013. DOI:10.4028/www.scientific.net/AST.77.285

[6] H. G. Kim, D. W. Hwang, and J. S. Lee, "An Undoped, Single-Phase Oxide Photocatalyst Working under Visible Light," *J. Am. Chem. Soc*., vol. 126, no. 29, pp. 8912-8913, 2004. DOI:10.1021/ja049676a

[7] M. Oshikiri, N. Boero, J. Ye, Z. Zou, and G. Kido, "Electronic Structures of Promising Photocatalysts $InMO_4$ (M=V, Nb, Ta) and $BiVO_4$ for Water Decomposition in The Visible Wavelength Region," *J. Chem. Phys*., vol. 117, no. 15, pp. 7313-7318, DOI:10.1063/1.1507101

[8] J. Tang, Z. Zou, J. Ye, "Efficient Photocatalytic Decomposition of Organic Contaminants over $CaBi_2O_4$ under Visible–Light Irradiation," *Angew. Chem. Int. Ed. Engl*., vol. 43, no. 34, pp. 4463-4466, 2004. DOI: 10.1002/anie.200353594

[9] H. Tong, S. Ouyang, Y. Bi, N. Uwezama, M. Oshikiri, and J. Ye, "Nano-Photocatalytic Materials: Possibilities and Challenge," *Adv. Mater*., vol. 24, no. 2, 2012. DOI: 10.1002/adma.201102752

[10] X. Liu, L. Xu, Y. Huang, C. Qin, L. Qin, and H. J. Seo, "Improved Photochemical Properties of Aurivillius $Bi_5Ti_3FeO_{15}$ with Partial Substitution of Ti^{4+} with Fe^{3+}," *Ceram. Int*., vol. 43, no. 5, pp. 12372-12380, 2017. DOI: 10.1016/j.ceramint.2017.06.103

[11] R. K. Agustina, D. Suheriyanto, and P. Anton, "The Molten Salt Synthesis of Vanadium-Doped $Bi_4Ti_3O_{12}$ Using Single Salt NaCl," *Jurnal Kartika Kimia*, vol. 3, pp. 19-24, 2020. DOI**:** 10.26874/jkk.v3i1.50

[12] Y. Yang, Q. Chen, Z. Yin, and J. Li, "Study on The Photocatalytic Activity of $K_2La_2Ti_3O_{10}$ Doped with Vanadium (V)," *J. Alloys Compd.*, vol. 488, no. 1, pp. 364-369, 2009. DOI: 10.1016/j.jallcom.2009.08.136

[13] C. N. R. Rao, "*Solid State Chemistry*," vol. 4. Singapore; World Scientific Publishing, 1995.

[14] J. Tellier, P. Boullay, M. Manier, and D. Mercurio. "A Comperative Study of The Aurivillius Phase Ferroelectrics $CaBi_4Ti_4O_{15}$ and $BaBi_4Ti_4O_{15}$," *J. Solid State Chem.,* vol. 177, no. 6, pp. 1829-1837, 2004. DOI: 10.1016/j.jssc.2004.01.008

[15] C. L. Diao, J. B. Xu, H. W. Zheng, L. Fang, Y. Z. Gu, and W. F. Zhang, "Dielectric and Piezoelectric Properties of Cerium Modified $BaBi_4Ti_4O_{15}$ Ceramics," *Ceram. Int*., vol. 39, no. 6, pp. 6991-6995, 2013. DOI:10.1016/j.ceramint.2013.02.036

[16] J. D. Bobic, M. M. V. Petrovic, and B. D. Stojanovic, "Aurivillius $BaBi_4Ti_4O_{15}$ Based Compounds: Structures, Synthesis, and Properties," *Process.*

Appl. Ceram., vol. 7, no. 3, pp. 97-110, 2013.
DOI: 10.2298/PAC1303097B

[17] W. Qi, Y. Wang, J. Wu, Z. Hu, C. Jia, and H. Zhang, "Relaxor Ferroelectric and Photocatalytic Properties of $BaBi_4Ti_4O_{15}$," *Adv. Appl. Ceram.*, vol. 118, no. 7, pp. 418-424, 2019.
DOI: 10.1080/17436753.2019.1634943

[18] A. Kudo, dan Y. Miseki, "Heterogenous Photocatalyst Materials for Water Splitting," *Chem. Soc. Rev*., no. 38, pp. 253-278, 2008.
DOI: 10.1039/B800489G

[19] A. D. Paola, E. García-López, S. Ikeda, G. Marcì, B. Ohtani, and L. Palmisano, "Photocatalytic Degradation of Organic Compounds in Aqueous Systems by Transition Metal Doped Polycrystalline TiO_2," *Catal. Today*, vol. 75, no. 1-4, pp. 87–93, 2002.
DOI:10.1016/s0920-5861(02)00048-2

[20] A. Z. Simoes, B. Stojanovic, M. A. Ramirez, A. A. Cavelheiro, E. Longo, and J. A. Varela, "Lanthanum Doped $Bi_4Ti_3O_{12}$ Prepared by The Soft Chemical Method: Rietveld Analysis and Piezoelectric Properties," *Ceram. Inter*., vol. 34, no. 2, pp. 257-261, 2008.
DOI: 10.1016/j.ceramint.2006.09.019

[21] C. Chen, K. Song, W. Bei, J. yang, Y. Zhang, P. Xiang, M. Qin, X. Tang, and J. Chu, "Effect of Nb and More Fe Ions Co-Doping on The Microstructures, Magnetic, and Piezoelectric Properties of Aurivillius $Bi_5Ti_3FeO_{15}$ Phases," *J. Appl. Phys*., vol. 120, no. 21, pp. 1-9, 2016.
DOI: 10.1063/1.4971256

[22] X. Liu, L. Xu, Y. Huang, C. Qin, L. Qin, and H. J. Seo, "Improved Photochemical Properties of Aurivillius $Bi_5Ti_3FeO_{15}$ with Partial Substitution of Ti^{4+} with Fe^{3+}," *Ceram. Int.*, vol. 43, no. 5, pp. 12372-12380, 2016.
DOI: 10.1016/J.CERAMINT.2017.06.103

[23] J. Hou, R. Cao, Z. Wang, S. Jiao, and H. Zhu, "Chromium-Doped Bismuth Titanate Nanosheets as Enhanced Visible-Light Photocatalyst with A High Percentage of Reactive {110} Facets," *J. Mater. Chem.*, vol. 21, no. 20, pp. 7296-7301, 2011.
DOI: 10.1039/C0JM04374E

[24] D. Gu. Y. Qin, Y. Wen, T. Li, L. Qin, and H. J. Seo, "Electronic Structure and Optical Properties of V-Doped $Bi_4Ti_3O_{12}$ Nanoparticles," *J. Alloys Compd*., vol. 695, pp. 2224-2231, 2016.
DOI: 10.1016/j.jallcom.2016.11.071

[25] X. Lin, Q. Guan, Y. Zhang, T. Liu, C. Zou, C. Liu, and H. Zhai, "Visible Light Photocatalytic Properties of $Bi_{3.25}Eu_{0.75}Ti_3O_{12}$ Nanowires," J. *Phys. Chem. Solids*., vol. 74, no. 9, pp. 1254-1262, 2013.
DOI: 10.1016/j.jpcs.2013.04.001

[26] E. V. Ramana, N. V. Prasad, D. M. Tobaldi, J. Zavasnik, M. Singh, M. J. Hortiguela, M. Seabra, G. Prasad, and M. A. Valente, "Effect of Samarium and Vanadium co-Doping on Strucutre, Ferroelectric and Photocatalytic Properties of Bismuth Titanate," *RSC Adv*., vol. 7, no. 16, pp. 9680-9692, 2017.
DOI: 10.1039/C7RA00021A

[27] W. C. Ferreira, G. L. C. Rodrigues, B. S. Araujo, F. A. A. Aguiar, A. N. A. A. Silva, P. B. A. Fechine, C. W. A. Paschoal, and A. P. Ayala, "Pressure Induced Structural Phase Transition in The Multiferroic Four-Layer Aurivillius Ceramic $Bi_5FeTi_3O_{15}$," *Ceram. Int.*, vol. 46, pp. 18056-18062, 2020.
DOI: 10.1016/j.ceramint.2020.04.122

[28] Z. Zhao, X. Li, H. Ji, and M. Deng, "Formation Mechanism of Plate-Like $Bi_4Ti_3O_{12}$ Particles in Molten Salt Fluxes," *Integr. Ferroelectr*, vol. 154, no. 154, pp. 37-41, 2014.
DOI: 10.1080/10584587.2014.904705

[29] C. Y. Kim, T. Sekino, and K. Nihara, "Synthesis of Bismuth Sodium Titanate Nanosized Powders by Solution/Sol-Gel Process," *J. Am. Ceram., Soc.,* vol. 86, no. 9, pp. 1464-1467, 2003.
DOI: 10.1111/j.1151-2916.2003.tb03497.x

[30] P. Pookmanee, P. Uriwilast, and S. Phanichpant, "Hydrothermal Synthesis of Fine Bismuth Titanate Powders," *Ceram. Int.*, vol. 30, no. 70, pp. 1913-1915, 2004.
DOI:10.1016/j.ceramint.2003.12.043

[31] C. Sikaladis, "*Advances in Ceramics: Synthesis and Characterization, Processing and Specific Application*," Rijeka: In Tech, 2011.

[32] Z. Lou, H. Minglong, W. Ruikun, Q, Weiwei, Z. Deijan, and C. Changel, "Large-Scale Synthesis of Monodisper Magnessium Ferrite via an Enviromentally Friendly Molten Salt Route," *Inorg. Chem.*, vol. 53, no. 4, pp. 2053-2057, 2014.
DOI: 10.1021/ic402558t

[33] Y. Mao, T. Tran, X. Guo, J. Y. Huang, C. K. Shih, K. L. Wang, and J. P. Chang, "Environmentally Friendly Methodologies of Nanostructure Synthesis," *Small,* vol 3, no. 7: 1122-1139. 2007.
DOI: 10.1002/smll.200700048.

[34] Y. Yu, S. Wang, W. Li, and Z. Chen, "Low Temperature Synthesis of LaB_6 Nanoparticles by a Molten Salt Route," *Powder Technol.*, vol. 323, pp. 203-207, 2018.
DOI: 10.1016/J.POWTEC.2017.09.049

[35] Y. Mao, X. Guo, J. Y. Huang, K. L. Wang, and J. P. Chang, "Luminescent Nanocrystals with $A_2B_2O_7$ Composition Synthesized by A Kinetically Modified Molten Salt Method," *J. Phys. Chem. C.*, vol. 113, no. 4, pp. 1204-1208, 2009.
DOI: 10.1021/jp807111h

[36] X. Liu, N. Fechler, and M. Antonietti, "Salt Melt Synthesis of Ceramics, Semiconductors and Carbon Nanostructures," *Chem. Soc. Rev.,* vol. 42, no. 21, pp. 8237-8265, 2013.
DOI: 10.1039/C3CS60159E

[37] Y. Chang, J. Wu, M. Zhang, E. Kupp, and G. L. Messing, "Molten Salt Synthesis of Morphology Controlled α-Alumina Platelets," *Ceram. Int.*, vol. 43, no.15, pp. 12684-12688, 2017.
DOI: 10.1016/j.ceramint.2017.06.150

[38] J. P. Zuniga, M. Abdou, S. K. Gupta, and Y. Mao, "Molten-Salt Synthesis of Complex Metal Oxides Nanoparticles," *J. Vis. Exp.*, vol. 140, pp. 1-7, 2018.
DOI:10.3791/58482

[39] J. Huang, L. Lihua, Y. Gu, and Q. L. Li, "Influences of Progressing Parameters on Flake $BaBi_4Ti_4O_{15}$ Powder Synthesized by Molten Salt Synthesis Method," *Adv. Mat. Res*., vol. 335-336, pp. 704-707, 2011.
DOI: 10.4028/www.scientific.net/AMR.335-336.704

[40] T. Kimura and Y. Yoshida, "Origin of Texture Development in Barium Bismuth Titanate Prepared by The Templated Grain Growth Method," *J. Am. Ceram. Soc*., vol. 89, no. 3, pp. 869-874, 2006.
DOI: 10.1111/j.1551-2916.2006.00846.x

[41] H. Irie, M. Miyayama, T. Kudo, "Enhanced Ferroelectric Properties of V-Doped $BaBi_4Ti_4O_{15}$ Single Crystal," *Jpn. J. Appl. Phys*., vol. 40, no. 1, pp. 239-243.
DOI:10.1143/JJAP.40.239

[42] T. Badapanda, P. Nayak, S. R. Mishra, R. Harichandan, and P. K. Ray, "Investigation of Temperature Variant Dielectric and Conduction Behaviour of Strontium Modified $BaBi_4Ti_4O_{15}$ Ceramic," *J. Mater. Sci. Mater*., vol. 30, no. 3, pp. 1-9, 2019.
DOI:10.1007/s10854-019-00678-6

[43] H. Maulidianingtiyas, A. D. Prasetiyo, F. Haikal, I. N. Cahyo, V. N. Istighfarini, and A. Prasetyo, "Pengaruh Penggantian Kation-*A*/Sr oleh Ba pada Morfologi Partikel $Ba_xSr_{(1-x)}TiO_3$ (x = 0; 0,2; 0,4; 0,6; 0,8) Hasil Sintesis dengan Metode Lelehan Garam," *Alchemy*, vol. 17, no. 2, pp. 211-218, 2021.
DOI:
10.20961/alchemy.17.2.48554.211-218

[44] P. Makula, M. Pacia, and W. Mayck, "How to Correctly Determine The Band Gap Energy of Modified Semiconductor Photocatalysts Based on UV-Vis Spectra," *J. Phys. Chem. Lett*., vol. 9, no. 23, pp. 6814-6817, 2018.
DOI:10.1021/acs.jpclett.8b02892

[45] T. Kocak, L. Wu, J. Wang, U. Savaci, S. Turan, and X. Zhang, "The Effect of Vanadium Doping on The Cycling Performance of $LiNi_{0,5}Mn_{1,5}O_4$ Spinel Cathode for High Voltage Lithium-Ion Batteries," *J. Electroanal. Chem.*, vol. 881, no. 47, pp. 114926-114963, 2021.
DOI: 10.1016/j.jelechem.2020.114926

[46] Y. Chen, J. Xu, S. Xie, Z. Tan, R. Nie, Z. Guan, and J. Zhu, "Ion Doping Effects on the Lattice Distortion and Interlayer Mismatch of Aurivillius-Type Bismuth Titanate Compounds," *Materials*., vol. 11, no. 5, pp. 821-835, 2018.
DOI: 10.3390/ma11050821

[47] N. Aini, R. Ningsih, D. Maulina, F. F. Lami', and S. N. Chasanah, "Visible Light Driven Photocatalyst of Vanadium (V^{3+}) Doped TiO_2 Synthesized Using Sonochemical Method," *Mater. Sci. Eng*., vol. 333, no. 1, pp. 1-5, 2018.
DOI:10.1088/1757-899X/333/1/012020

[48] T. S. Kim, K. W. Kim, M. K. Jeon, C. H. Jung, and S. I. Woo, "Effect of Vanadium Content on Remanent Polarization in Bismuth Titanate Thin Films Prepared by Liquid Source Misted Chemical Deposition," *Appl. Phys. Lett*., vol. 90, no. 4, pp. 042912-042915, 2007.
doi:10.1063/1.2432226

[49] A. Kikuchihara, F. Sakurai, and T. Kimura, "Preparation of Platelike $NaNbO_3$ Particles by Single Step Molten Salt Synthesis," *J. Am. Ceram. Soc.*, vol. 95, no. 5, pp. 1556-1562, 2012.
DOI:10.1111/j.1551-2916.2012.05095.x

[50] T. Wang and T. Xu, "Effects of Vanadium Doping on Microstructures and Optical Properties of TiO_2," *Ceram. Int.*, vol. 43, no. 1, pp. 1558-1564, 2017.
DOI: 10.1016/j.ceramint.2016.10.132

[51] D. Gu, Y, Qin, Y. Wen, T. Li, L. Qin, and H. J. Seo, "Electronic Structure and Optical Properties of V-Doped $Bi_4Ti_3O_{12}$ Nanoparticles," *J. Alloys Compd*., vol. 695, pp. 2224-2231, 2016.
DOI:10.1016/j.jallcom.2016.11.071

[52] H. X. Zhu, X. H. Wang, D. F. Zhou, H. Jiang, and X. M. Liu, "First-Principles Study on Electronic, Magnetic Properties and Optical Absoprtion of Vanadium Doped Rutile TiO_2," *Phys. Lett. A*., vol. 384, no. 26, pp. 1-7, 2020.
DOI: 10.1016/j.physb.2009.01.014

[53] Q. Sun, B. R. McBride, and Y. Liu, "(N^{3-}, M^{5+}) Co-Doping Strategies for The Development of TiO_2-Based Visible Light Catalyst," *Res. Rev. Electrochem.*, vol. 8, no. 1, pp. 1-10, 2017.

[54] B. Tian and C. Li, "Flame Sprayed V-Doped TiO_2 Nanoparticles with Enhaced Photocatalytic Activity under Visible Light Irradiation," *Chem. Eng. J.*, vol. 151, no. 1-3, pp. 220-227, 2019.
DOI: 10.1016/j.cej.2009.02.030